

INCIPIENT FAULT SEVERITY ESTIMATION USING LOCAL MAHALANOBIS DISTANCE

Junjie YANG and Claude DELPHA

Université Paris Saclay, CNRS, CentraleSupélec, Laboratoire des Signaux et Systèmes
UMR 8506, Plateau du Moulon, 3 Rue Joliot Curie, Gif sur Yvette, France

ABSTRACT

Recently, the Local Mahalanobis Distance (LMD) technique was proposed for incipient fault detection, which was shown to be sensitive, robust and distribution assumption-free. Further, this paper explicitly establishes the relation between fault severity and LMD index to take advantage of those excellent characteristics for fault severity estimation. The performance of the estimation model is evaluated based on a benchmark case of Continuous-flow Stirred Tank Reactor (CSTR) process, which shows a high accuracy even for tiny deviation of signal and large signal-to-noise ratio.

Index Terms— Fault severity estimation, Incipient fault diagnosis, local Mahalanobis distance, CSTR

1. INTRODUCTION

Fault diagnosis is a hot topic in the signal processing domain with wide applications like chemical manufacturing, electrical system, and mechanical process [1–4]. For process monitoring, a fault defined as “*the unpermitted deviation of at least one parameter from an acceptable condition*” can be further distinguished according to its time-dependency, such as incipient fault and abrupt fault [5,6]. In contrast to the considerable progress of the research on abrupt fault diagnosis, the studies of incipient fault diagnosis are more tedious. The main difficulty of this topic lies in confusion between noise and tiny deviation of signals, which actually requires higher sensitivity and stronger robustness of diagnosis methodologies [7,8].

To prevent a fault from developing into a severe system breakdown, early detection of incipient fault is crucial. It raises the great interest of high sensitive fault evaluation criteria for univariate and multivariate data. As an example, recent methods based on, Kullback-Leibler Divergence (KLD) [9–11] or Jensen-Shannon Divergence (JSD) [12,13] were proposed. For multivariate data, these divergence-based methods often include a data preprocessing operation with dimension reduction techniques, like principal component analysis. The divergence values are then calculated based on the estimated probability density function of the retained components and used as a diagnosis index. This may induce information loss

detrimental for diagnosis. High sensitive multivariate statistical process monitoring approaches were also developed, such as Canonical Variate Dissimilarity Analysis (CVDA) [14,15] and Local Mahalanobis Distance Analysis (LMDA) [8,16]. In particular, LMDA outperforms several other approaches for its good performances in terms of high sensitivity, small detection delay and free distribution assumption.

After fault detection, additional fault analyses, such as faulty variable isolation and fault severity estimation, are also necessary for fault-tolerant control or Remaining Useful Life (RUL) prediction [2,17]. In fact, a number of fault severity estimation approaches for particular systems have been proposed, and their effectiveness was verified [18,19]. However, those specific-designed approaches usually suffer from weak generalization capability. Therefore, general methods were developed based on Reconstruction-Based Contribution (RBC) [20], KLD [21,22], and JSD [12,13]. Despite significant progress, most fault severity estimation methodologies still have drawbacks like low accuracy and weak robustness to noise. Furthermore, the performance evaluation concerning different noise levels is usually missing in the literature.

This paper studies the relevance between fault severity and LMD index and then develops an analytical model based on LMD for fault severity estimation. CSTR process is then used as a case study to evaluate its accuracy performance. The contribution of this work is twofold. First, an analytical model for fault severity estimation is developed based on LMD and its good properties (sensitivity, robustness, few assumptions). The advantages of LMD help the estimation model to lead to accurate results. Secondly, based on CSTR process, this work comprehensively evaluates the estimation performance, considering different noise levels, fault severity values and faulty scenarios. The impact of those factors is exhibited, which points out potential ways for future improvement. The rest of the paper is organized as follows. Section 2 revisits the LMD. Then, the analytical model for fault severity estimation is introduced in section 3. So, the performance evaluation is carried out in section 4. Finally, section 5 concludes the paper.

2. LMD REVISITED

LMD is an unsupervised technique proposed to handle unknown distributed data and improve the detection sensitivity

The authors would like to thank China Scholarship Council for funding.

of incipient fault. It aims at specifying an optimal healthy region based on the given fault-free data, which is called healthy domain approximation. By modeling the healthy border as multiple hyperspheres, it can be represented by a series of anchors and a radius. Based on the anchors set, LMD is calculated as an index optimally indicating the similarity of a new sample and the healthy historical data.

The theoretical analysis of LMD and its applications to incipient fault detection were pioneered in [8, 16]. In the following, we briefly revisit and remind the LMD's definition with its training process for better understanding and then give the basics for developing the estimation.

2.1. Local Mahalanobis Distance

Let us consider two sample vectors \mathbf{A}, \mathbf{B} coming from the same distribution with mean vector $\boldsymbol{\mu}$ and covariance matrix $\boldsymbol{\Sigma}$. The multivariate Mahalanobis distance between \mathbf{A} and \mathbf{B} is given as:

$$d_M(\mathbf{A}, \mathbf{B}) = \sqrt{(\mathbf{A} - \mathbf{B})^T \boldsymbol{\Sigma}^{-1} (\mathbf{A} - \mathbf{B})} \quad (1)$$

Then, LMD is defined as the closest Mahalanobis distance from a sample to a predefined healthy domain, where the latter is approximated and represented as an anchors set in a training process. Let $S = \{\mathbf{C}_1, \dots, \mathbf{C}_k, \dots, \mathbf{C}_\kappa\}$ be the anchor set with κ elements, the LMD of a given sample vector \mathbf{x} is:

$$D(\mathbf{x}; S) = \min_k \{d_M(\mathbf{x}, \mathbf{C}_k) | \mathbf{C}_k \in S\} \quad (2)$$

Thus, the corresponding local anchor $\mathcal{A}(\mathbf{x})$ is written:

$$\mathcal{A}(\mathbf{x}) = \arg \min_k \{d_M(\mathbf{x}, \mathbf{C}_k) | \mathbf{C}_k \in S\} \quad (3)$$

These anchors are then used to evaluate new test samples in a diagnosis process.

Obviously, LMD is always a positive or null value. Close to zero, its value indicates the healthy behavior of the corresponding sample. With large values it indicates a potential faulty behavior. In fact, benefiting from the local analysis of samples' spatial position relative to the healthy domain, LMD can sensitively indicate the change of sample's pattern (healthy to faulty). Moreover, additionally to fault detection, it allows further analysis of faulty behaviors as the fault severity estimation. Our present work focus on this purpose.

2.2. LMD for training

For LMD calculation, the training process generating anchors set from historical fault-free samples is first computed. The training process aims at extracting critical spatial information and removing redundancy from the original healthy samples. A distance-based down-sampling algorithm was first proposed to identify and merge geometrically close samples as an anchor [8]. Its improvement for better robustness to

outliers considers the local density information. Note that the proposed algorithm is not a simple clustering-like method but a crucial part of the LMD framework for optimization. Here, we summarize the up-to-date anchors-generation algorithm as Algorithm 1 that is considered in the estimation study.

Algorithm 1 Anchor-generation algorithm

Input: Fault-free samples $\mathbf{X}^* = \{\mathbf{x}_i\}_{i=1}^K$, region radius γ , minimum number of local samples η

Output: Anchors set S

```

1:  $\boldsymbol{\mu} \leftarrow \frac{\sum_{i=1}^K \mathbf{x}_i}{K}$ 
2:  $\mathbf{C}_1 \leftarrow \boldsymbol{\mu}$ 
3:  $\boldsymbol{\Sigma} \leftarrow \text{cov}(\mathbf{X}^*, \mathbf{X}^*)$ 
4:  $d_M(\mathbf{x}_i) \leftarrow \sqrt{(\mathbf{x}_i - \boldsymbol{\mu})^T \boldsymbol{\Sigma}^{-1} (\mathbf{x}_i - \boldsymbol{\mu})}$ 
5: Rearrange fault-free samples as  $\mathbb{Q}$  in ascending order according to  $d_M(\mathbf{x}_i)$ 
6:  $k \leftarrow 2$ 
7: repeat
8:   Take one sample  $\mathbf{x}_i$  from  $\mathbb{Q}$ 
9:   Find out  $Z_k = \{\mathbf{x}_l | d_M(\mathbf{x}_i, \mathbf{x}_l) < \gamma, l > i, \mathbf{x}_l \in \mathbb{Q}\}$ 
10:   $n_k \leftarrow$  samples number in  $Z_k$ 
11:  if  $n_k < \eta$  then Continue
12:  end if
13:   $\mathbf{C}_k \leftarrow \frac{1}{n_k} \sum_{q=1}^{n_k} \mathbf{x}_q (\mathbf{x}_q \in Z_k)$ 
14:  Remove  $Z_k$  from  $\mathbb{Q}$ 
15:   $k \leftarrow k + 1$ 
16: until  $\mathbb{Q}$  is empty
17:  $S \leftarrow \{\mathbf{C}_1, \dots, \mathbf{C}_k, \dots, \}$ 
18: return  $S$ ;
```

To obtain an effective anchors set for LMD calculation, η should be at first tuned according to the strength of outliers. Generally, a large η value should be considered when data contain large numbers of outliers. Then region radius γ can be optimized by minimizing the following cost function:

$$\text{Err} = \sum_{i=1}^K D(\mathbf{x}_i; S), \quad (\mathbf{x}_i \in \mathbf{X}^*) \quad (4)$$

The optimal anchors set marks the critical spatial position of the healthy domain and also helps to keep high computational efficiency and robustness to outliers. In the following fault severity estimation procedure, the optimal anchors set is directly used for LMD calculation.

3. FAULT SEVERITY ESTIMATION

Let's consider a data matrix $\mathbf{X}_{[N \times m]}$ with m variables and N observations. A fault is supposed to occur at b and affect the c^{th} variable. In other words, the last $N - b + 1$ observations of the c^{th} variable are faulty. Then, according to the definition of incipient fault, sample vector \mathbf{x}_i can be decomposed into three parts, the fault-free samples \mathbf{x}_i^* , the fault component \mathbf{F}_i

and a noise component \mathbf{v}_i , such as:

$$\mathbf{x}_i = \mathbf{x}_i^* + \mathbf{F}_i + \mathbf{v}_i \quad (5)$$

where $\mathbf{F}_i = [0, \dots, \Delta_i^c, \dots, 0]$, and Δ_i^c is fault amplitude.

In literature works [13,22], Δ_i^c was characterized as a constant in small duration, which is simple but lacks the fault evolution information. In order to theoretically study the revolution of fault amplitude depending on time and keep the simplicity of a model, we develop the first-order approximation of faulty behavior, such as:

$$\Delta_i^c = \delta \cdot (i - b + 1) \cdot T_e, \quad (i \geq b) \quad (6)$$

where δ is the fault severity regarded as a constant, and T_e is the sampling time.

To explicitly establish the relation between δ and LMD, we develop Eq(2) to:

$$\begin{aligned} D(\mathbf{x}_i, S) &= d_M(\mathbf{x}_i, \mathcal{A}(\mathbf{x}_i)) \\ &= \sqrt{[\mathbf{x}_i - \mathcal{A}(\mathbf{x}_i)]^T \Sigma^{-1} [\mathbf{x}_i - \mathcal{A}(\mathbf{x}_i)]} \\ &= \|\mathbf{x}_i - \mathcal{A}(\mathbf{x}_i)\|^T \Sigma^{-\frac{1}{2}} \|_2 \end{aligned} \quad (7)$$

where $\|\cdot\|_2$ is the L^2 norm. Then, substituting Eq(5) into Eq(7), we have:

$$D(\mathbf{x}_i, S) = \|\mathbf{x}_i^* + \mathbf{F}_i + \mathbf{v}_i - \mathcal{A}(\mathbf{x}_i)\|^T \Sigma^{-\frac{1}{2}} \|_2 \quad (8)$$

For simplicity, the following notations are used:

$$\boldsymbol{\zeta}_i = \mathbf{x}_i^* + \mathbf{v}_i - \mathcal{A}(\mathbf{x}_i) \quad (9)$$

$$\boldsymbol{\zeta}'_i = \boldsymbol{\zeta}_i \Sigma^{-\frac{1}{2}} = [\zeta'_{i1}, \dots, \zeta'_{ij}, \dots, \zeta'_{im}] \quad (10)$$

$$\Sigma^{-\frac{1}{2}} = \begin{bmatrix} \varsigma_{11} & \dots & \varsigma_{1j} & \dots & \varsigma_{1m} \\ \vdots & & \vdots & & \vdots \\ \varsigma_{j1} & \dots & \varsigma_{jj} & \dots & \varsigma_{jm} \\ \vdots & & \vdots & & \vdots \\ \varsigma_{m1} & \dots & \varsigma_{mj} & \dots & \varsigma_{mm} \end{bmatrix} \quad (11)$$

Then Eq(8) is simplified and developed as:

$$D^2(\mathbf{x}_i; S) = \|\boldsymbol{\zeta}'_i\|_2^2 + 2\Delta_i^c \sum_{j=1}^m \zeta'_{ij} \varsigma_{cj} + \Delta_i^{c2} \sum_{j=1}^m \varsigma_{cj}^2 \quad (12)$$

Eq(12) can be further developed based on the first-order approximation model by substituting Eq.(6)

Since ζ'_{ij} in Eq(13) is unknown, δ can not be calculated directly through this equation. However, Eq(13) indicates that the square of LMD is a function of sample index i . Let

$$D^2(\mathbf{x}_i; S) = a_2 i^2 + a_1 i + a_0 \quad (14)$$

where

$$a_2 = \delta^2 T_e^2 \sum_{j=1}^m \varsigma_{cj}^2 \quad (15)$$

$$a_1 = 2\delta T_e \sum_{j=1}^m \zeta'_{ij} \varsigma_{cj} + 2(1-b)\delta^2 T_e^2 \sum_{j=1}^m \varsigma_{cj}^2 \quad (16)$$

$$a_0 = 2(1-b)\delta T_e \sum_{j=1}^m (\varsigma_{cj}^2 + \zeta'_{ij} \varsigma_{cj}) + \|\boldsymbol{\zeta}'_i\|_2^2 \quad (17)$$

As $D^2(\mathbf{x}_i; S)$ has been calculated previously for detection and i is known, the coefficients a_0, a_1, a_2 can be easily estimated by the polynomial curves fitting technique. More accurately, the estimation is implemented by minimizing the sum of squared error between the true output D^2 and the estimated one based on samples from b to N . Let

$$\mathbf{W} = [a_0, a_1, a_2] \quad (18)$$

$$\Xi^T = \begin{bmatrix} 1 & \dots & 1 & \dots & 1 \\ b & \dots & i & \dots & N \\ b^2 & \dots & i^2 & \dots & N^2 \end{bmatrix} \quad (19)$$

$$\mathbf{Y} = [D^2(\mathbf{x}_b; S), \dots, D^2(\mathbf{x}_i; S), \dots, D^2(\mathbf{x}_N; S)]^T \quad (20)$$

The coefficients vector \mathbf{W} is calculated as:

$$\mathbf{W} = (\Xi^T \Xi)^{-1} \Xi^T \mathbf{Y} \quad (21)$$

Then the estimated fault severity $\hat{\delta}$ is finally obtained as:

$$\hat{\delta} = \sqrt{\frac{a_2}{T_e^2 \sum_{j=1}^m \varsigma_{cj}^2}} \quad (22)$$

4. PERFORMANCE ANALYSIS

A benchmark case Continuous-flow Stirred Tank Reactor (CSTR) process was introduced to validate the effectiveness of fault severity estimation. To that end, the CSTR model was used to generate data with 7 variables and simulate 7 additive faults caused by sensor drifts [15]. Those faulty scenarios were labeled as F_1 to F_7 , respectively, with subscripts indicating the number of faulty variables.

In the validation procedure, signals were sampled every 1 minute for a total duration of 20 hours. In other words, the sampling time is $T_e = 1$ (min) and the samples number is $N = 1200$. Then, a fault was introduced at 1000 minutes for each faulty scenario, viz. $b = 1000$. In the training process of the method, given the minimum number of local samples $\eta = 2$, the optimization procedure was activated and obtained the optimal region radius $\gamma^{opt} = 1.448$ and 224 anchors.

If we consider F_4 as an example, Fig.1 displays the estimated fault severity results for different values of δ . Basically, the evolution of $\hat{\delta}$ shows asymptomatic consistency of the real value when δ increases from 3×10^{-4} . For extremely small values of δ , ($\delta < 3 \times 10^{-4}$), the result starts with an opposite evolution tendency and finally steadies at a small positive value with δ decreasing to 0. In fact, for such trick cases, signal's tiny changes are easily confused with noise, resulting

$$\begin{aligned}
D^2(x_i; S) &= \|\zeta'_i\|_2^2 + 2\delta(i-b+1)T_e \sum_{j=1}^m \zeta'_{ij}\zeta_{cj} + [\delta(i-b+1)T_e]^2 \sum_{j=1}^m \zeta_{cj}^2 \\
&= (\delta^2 T_e^2 \sum_{j=1}^m \zeta_{cj}^2)_i^2 + 2[\delta T_e \sum_{j=1}^m \zeta'_{ij}\zeta_{cj} + (1-b)\delta^2 T_e^2 \sum_{j=1}^m \zeta_{cj}^2]i + 2(1-b)\delta T_e \sum_{j=1}^m (\zeta_{cj}^2 + \zeta_{ij}\zeta_{cj}) + \|\zeta'_i\|_2^2 \quad (13)
\end{aligned}$$

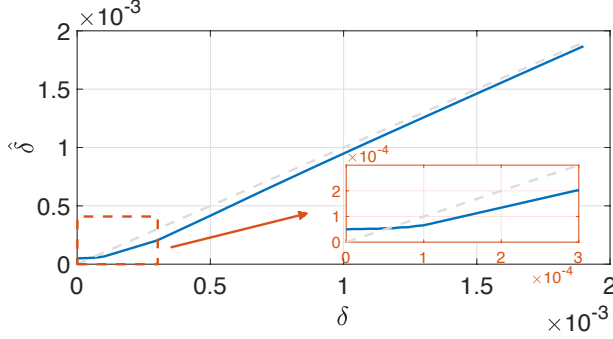


Fig. 1. Estimated fault severity result versus real value for F_4 with SNR = 30dB

in the weak estimating capability of typical methods. However, Fig.1 shows that the proposed method is still effective and able to obtain accurate results for tiny deviation.

To uniformly show the error between estimated and true fault severity value, we consider the relative error $\epsilon = \frac{\hat{\delta} - \delta}{\delta}$. Furthermore, fault severity is qualified by the signal-to-fault ratio (SFR) to eliminate the bias causing by different signal's power. To reveal the effect of true fault severity degree and noise strength on the method's performance, Fig.2 shows the relative error for F_4 with SFR changing from 0dB to 34dB (δ decrease) and SNR varying from 10dB to 50dB. For all noise conditions, relative error values show a similar revolution pattern where values first decrease and then increase. For example, when SNR = 30dB, the error keep a decreasing tendency until SFR > 25dB. For extremely small fault severity, like SFR > 25dB, the relative error keeps increasing along with SFR. It is because when δ increases $\hat{\delta}$ turns to a stable value and δ decreases. This result shows the degraded estimation performance for extreme small fault severity.

On the other hand, the estimation accuracy is also affected by noise. With noise strength decreasing (SNR increasing), the relative error gets close to 0 and evolves more gently, implying a potential improvement by removing noise.

Finally, to exhibit the performance evolution of different faulty scenarios, we show relative errors for F_1 to F_7 with SFR varying from 0dB to 40dB, as shown in Fig.3. Obviously, the evolution patterns of different faulty cases are similar. However, F_1 , F_4 and F_7 seem more trick than other cases for their dramatic degradation with δ increasing.

In summary, the proposed method is effective for fault

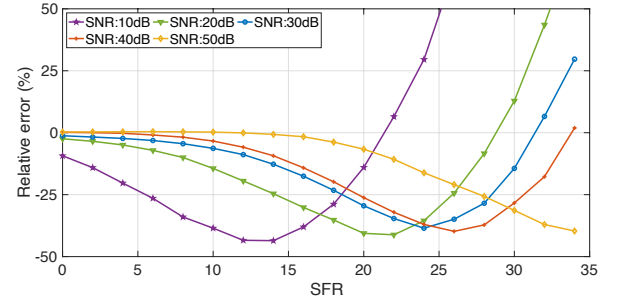


Fig. 2. Estimation relative error for F_4 with varying SFR and SNR

severity estimation of the CSTR process even though its performance slightly degrades for extremely small fault severity.

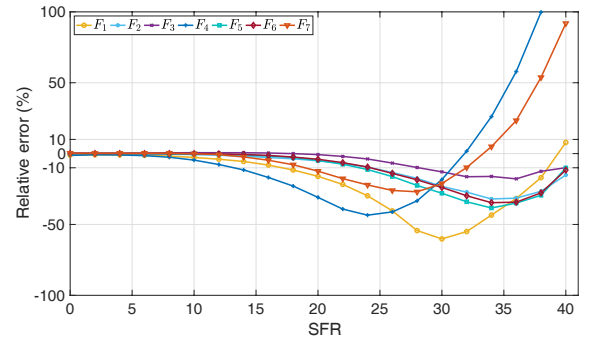


Fig. 3. Estimation relative errors for F_1 to F_7 with varying SFR and SNR = 30dB

5. CONCLUSION

This paper reveals that LMD is not only a sensitive measure for fault detection but also a crucial index benefiting fault severity estimation. Based on the first-order approximation model of incipient faults, fault severity can be analytically evaluated as a function of LMD. The intrinsic advantages of LMD, like robustness to noise and free-distribution assumption, are preserved in the fault severity estimation procedure. The performance evaluation result based on the CSTR process shows that the proposed method has high accuracy even for tiny fault severity values and different noise levels.

6. REFERENCES

- [1] R. Arunthavanathan, F. Khan, S. Ahmed, S. Imtiaz, and R. Rusli, "Fault detection and diagnosis in process system using artificial intelligence-based cognitive technique," *Computers & Chemical Engineering*, vol. 134, p. 106697, 2020.
- [2] X. Li, X. Yang, Y. Yang, I. Bennett, and D. Mba, "A novel diagnostic and prognostic framework for incipient fault detection and remaining service life prediction with application to industrial rotating machines," *Applied Soft Computing*, vol. 82, p. 105564, 2019.
- [3] M. Zhang, Z. Jiang, and K. Feng, "Research on variational mode decomposition in rolling bearings fault diagnosis of the multistage centrifugal pump," *Mechanical Systems and Signal Processing*, vol. 93, pp. 460–493, 2017.
- [4] U. Kruger and L. Xie, *Advances in statistical monitoring of complex multivariate processes: with applications in industrial process control*. Wiley, 2012.
- [5] R. Isermann, "Model-based fault-detection and diagnosis—status and applications," *Annual Reviews in control*, vol. 29, no. 1, pp. 71–85, 2005.
- [6] M. Basseville and I. V. Nikiforov, *Detection of abrupt changes: theory and application*. Prentice hall Englewood Cliffs, 1993, vol. 104.
- [7] C. Delpha and D. Diallo, "Incipient fault detection and diagnosis: a hidden information detection problem," in *24th International Symposium on Industrial Electronics (ISIE)*. IEEE, 2015, pp. 837–842.
- [8] J. Yang and C. Delpha, "An incipient fault diagnosis methodology using local Mahalanobis distance: Detection process based on empirical probability density estimation," *Signal Processing*, vol. 190, p. 108308, 2022.
- [9] J. Zeng, U. Kruger, J. Geluk, X. Wang, and L. Xie, "Detecting abnormal situations using the Kullback–Leibler divergence," *Automatica*, vol. 50, no. 11, pp. 2777–2786, 2014.
- [10] A. Youssef, C. Delpha, and D. Diallo, "An optimal fault detection threshold for early detection using Kullback–Leibler divergence for unknown distribution data," *Signal Processing*, vol. 120, pp. 266–279, 2016.
- [11] H. Chen, B. Jiang, and N. Lu, "An improved incipient fault detection method based on Kullback–Leibler divergence," *ISA transactions*, vol. 79, pp. 127–136, 2018.
- [12] X. Zhang, C. Delpha, and D. Diallo, "Performance of Jensen Shannon divergence in incipient fault detection and estimation," in *International Conference on Acoustics, Speech and Signal Processing (ICASSP)*. IEEE, 2019, pp. 2742–2746.
- [13] —, "Incipient fault detection and estimation based on Jensen–Shannon divergence in a data-driven approach," *Signal Processing*, vol. 169, p. 107410, 2020.
- [14] P.-E. P. Odiowei and Y. Cao, "Nonlinear dynamic process monitoring using canonical variate analysis and kernel density estimations," *IEEE Transactions on Industrial Informatics*, vol. 6, no. 1, pp. 36–45, 2009.
- [15] K. E. S. Pilario and Y. Cao, "Canonical variate dissimilarity analysis for process incipient fault detection," *IEEE Transactions on Industrial Informatics*, vol. 14, no. 12, pp. 5308–5315, 2018.
- [16] J. Yang and C. Delpha, "A local Mahalanobis distance analysis based methodology for incipient fault diagnosis," in *International Conference on Prognostics and Health Management (ICPHM)*. IEEE, 2021, pp. 1–8.
- [17] L. H. Chiang, E. L. Russell, and R. D. Braatz, *Fault detection and diagnosis in industrial systems*. Springer Science & Business Media, 2000.
- [18] Y. Wu, B. Jiang, and N. Lu, "A descriptor system approach for estimation of incipient faults with application to high-speed railway traction devices," *IEEE Transactions on Systems, Man, and Cybernetics: Systems*, vol. 49, no. 10, pp. 2108–2118, 2017.
- [19] V. Nguyen, D. Wang, J. Seshadrinath, A. Ukil, M. S. Krishna, S. Nadarajan, and V. Vaiyapuri, "A method for incipient interturn fault detection and severity estimation of induction motors under inherent asymmetry and voltage imbalance," *IEEE Transactions on Transportation Electrification*, vol. 3, no. 3, pp. 703–715, 2017.
- [20] H. Ji, X. He, J. Shang, and D. Zhou, "Incipient sensor fault diagnosis using moving window reconstruction-based contribution," *Industrial & Engineering Chemistry Research*, vol. 55, no. 10, pp. 2746–2759, 2016.
- [21] J. Harmouche, C. Delpha, and D. Diallo, "Incipient fault detection and diagnosis based on Kullback–Leibler divergence using principal component analysis: Part II," *Signal Processing*, vol. 109, pp. 334–344, 2015.
- [22] —, "Incipient fault amplitude estimation using KL divergence with a probabilistic approach," *Signal Processing*, vol. 120, pp. 1–7, 2016.